Egyptian Geophysical Society
EGS Journal, Vol. 20, No. 1, 19-35 (2022)

RESERVOIR CHARACTERIZATION OF KAREEM FORMATION IN NORTH GEISUM FIELD - GULF OF SUEZ-EGYPT

S. Ismail. and M.H. El Shayib*

Geology Department, Faculty of Science, Menoufiya University, Egypt.

* safwatismail54@yahoo.com

تقييم تكون خزان كريم فى حقل شمال جيسوم - خليج السويس - مصر

الخلاصة: يقع حقل نفط شمال جيسوم جنوب شرق خليج زيت في الجزء الجنوبي البحري من خليج السويس و يغطي مساحة حوالي ٣٠ كيلومتر مربع حيث توجد العديد من مصائد الهيدروكربون التي تنتج النفط من خزانات مختلفة من مختلف العصور الجيولوجية (العصر الطباشيري السفلي إلى الميوسين). تم تقسيم تكوين كريم في حقل نفط شمال جيسوم إلى مجموعتين (من أعلى إلى أسفل) شجر و رحمى.

تهدف هذه الدراسة إلى تقييم وتفسير المتغيرات البتروفيزيقيه لخصائص مكمن كريم والتي تمثلت من خلال توزيعها الرأسي والأفقي للآبار المدروسة.

تم تمثيل التوزيع العمودي للخواص البتروفيزيقيه من خلال عدد من علاقات التشبع الصخري لأعضاء الشجر والرحمي لكل بئر لإظهار التباين الرأسي للصخور والمسامية ومحتواها من الهيدروكربون و تم تمثيل التوزيع الأفقي للخواص البتروفيزيقيه مثل حجم المحتوى الطينى (Vsh) ، وتشبع بالهيدروكربون (Sh) ، والمسامية الكلية والفعالة وتم التمثيل بعدد من الخرائط.

أظهرت الدراسة الحالية أن السمك الطبقه المنتجه للخزان يتراوح بين ٦ و ١١٧ قدمًا وتتراوح المسامية الفعالة بين ١٢٪ و ٢٢,٥٪ ويتراوح محتوى الطين بين ٥٪ و ٢٢٪ والتشبع بالهيدروكربون ٥٥٪ و ٨٤٪ وهذا يشير إلى أن شجر ورحمي هم مكامن جيدة ذات إمكانات عالية لإنتاج النفط.

ABSTRACT: *North Geisum oil field is located southeast of the Zeit bay at the offshore southern part of Gulf of Suez; it covers an area of about 30 km^2 where many hydrocarbon traps producing oil from different reservoirs of different geological ages (Lower Cretaceous to the Miocene) are encountered.*

Kareem Formation in North Geisum oil field has been divided into two members (from top to bottom) Shagar and Rahmi members.

This study aims to evaluation of reservoir properties is the estimation of hydrocarbons in the porous zones encountered in the Miocene sequence Shagar Cap, Shagar Sand, Rahmi Clastics, Rahmi Sand beds from North Geisum oil field penetrated by four wells in the study area as revealed using schlumberger software, Interactive Petrophysics^{TM} (IP), Then data represented through vertical and horizontal distribution.

Vertical distribution of the petrophysical parameters were represented by a number of litho-saturation crossplots of the Kareem members for each well to show the vertical variation of the lithology, porosity and their hydrocarbon contents. Horizontal distribution of the petrophysical parameters such as shale volume (Vsh), fluid saturations (Sh), total and effective porosities (Φt and Φe) were represented by a number of isoparametric maps.

The estimated petrophysical parameters of the reservoir throughout the study area range between about 12% and 22.5 % for effective porosity, 5 % and 22 % for shale volume and between 55 % and 84% for hydrocarbon saturation. This indicates that Shagar and Rahmi sands in this field can be considered as good reservoirs with high potential for oil production.

1- INTRODUCTION

The Gulf of Suez is considered the most prolific oil province in Egypt, which is receiving the attention of many investigators due to the prospective potentials of hydrocarbon deposits that it contains. It constitutes a rift basin that was created by stretching and collapse of the crust. This process is often associated with hydrocarbon accumulation. Subsidence moves potential source rocks to depths suitable for oil and gas generation, and the stretching motion can produce structural traps in the fault blocks, which characterize rift basins (Schlumberger, 1995).

The Gulf of Suez continues to provide a focal point for the development of geological ideas and evolution of oil-related technology. New companies are entering the area and bringing a variety of exploration techniques. Well logging and borehole seismic surveying data are among the most effective tools in use which are utilized for exploring and evaluating the hydrocarbon reservoirs. They can be integrated together to better understand the reservoir of interest. The respective contribution of integrating both techniques is reflected obviously on the quality of the information of both techniques (Lashin et al., 2011).

North Geisum oil field is located southeast of the Zeit bay at the offshore southern part of Gulf of Suez, approximately 46 km north of Hurghada city east of

Zeit bay about 8 km. It covers an area of about 30 km^2. The study area is bounded between Latitudes 27° 40 ` 9.3`` to 27° 41` 8.357 N and Longitudes 33° 39`.585`` to 33° 39` 47.9`` E., southwestern Gulf of Suez, Egypt. (Fig. 1).

2-Materials and Methodology

The data used in this study for GC-3, GD-2, GW-9 and GC-8ST2 wells include:

- 20 3D seismic sections. Seismic sections were giving us wells to reveal and understand the regional structural feature affecting the area of interest.
-Well logs (composite, resistivity, self- potential, gamma ray, sonic, density, neutron, velocity and dip meter) which are used to evaluate the reservoir parameters.

Petrophysical evaluation of four selected wells GC-3, GD-2, GW-9 and GC-8ST2 in North Geisum oil field are determined analytically using a computer program that facilitates the different calculations (such as volume of shale, total and effective porosities and fluid saturations. The fore-mentioned petrophysical parameters for Kareem Formation, Shagar sand, Rahmi anhydrite, Rahmi Clastics and Rahmi Sand beds in the studied wells are presented vertically, in the form of litho-saturation crossplots. Normalized values for petrophysical parameter are presented laterally, in a number of iso-parametric maps. Thickness maps of the main stratigraphic units have been constructed to illustrate the impact of tectonics on the thickness variation and depositional evolution of the different stratigraphic units in the study area.

3-Stratigraphy

The lithostratigraphic units in the Gulf of Suez were subdivided into three major sequences related to the Miocene rifting event: a prerift succession (pre-Miocene or Paleozoic– Eocene), a synrift succession (Oligocene–Miocene), and a postrift succession (post-Miocene or Pliocene–Holocene) (Fig. 2). These units vary in lithology, thickness, areal distribution, depositional environment, and hydrocarbon importance (Alsharhan and Salah, 1997).

The Miocene in the Gulf of Suez is regionally classified into two main groups: the Lower Miocene Gharandal Group and the Middle Miocene Ras Malaab or Evaporite Group (Egyptian General Petroleum Corporation (EGPC, 1964 and Gawad et al., 1986).

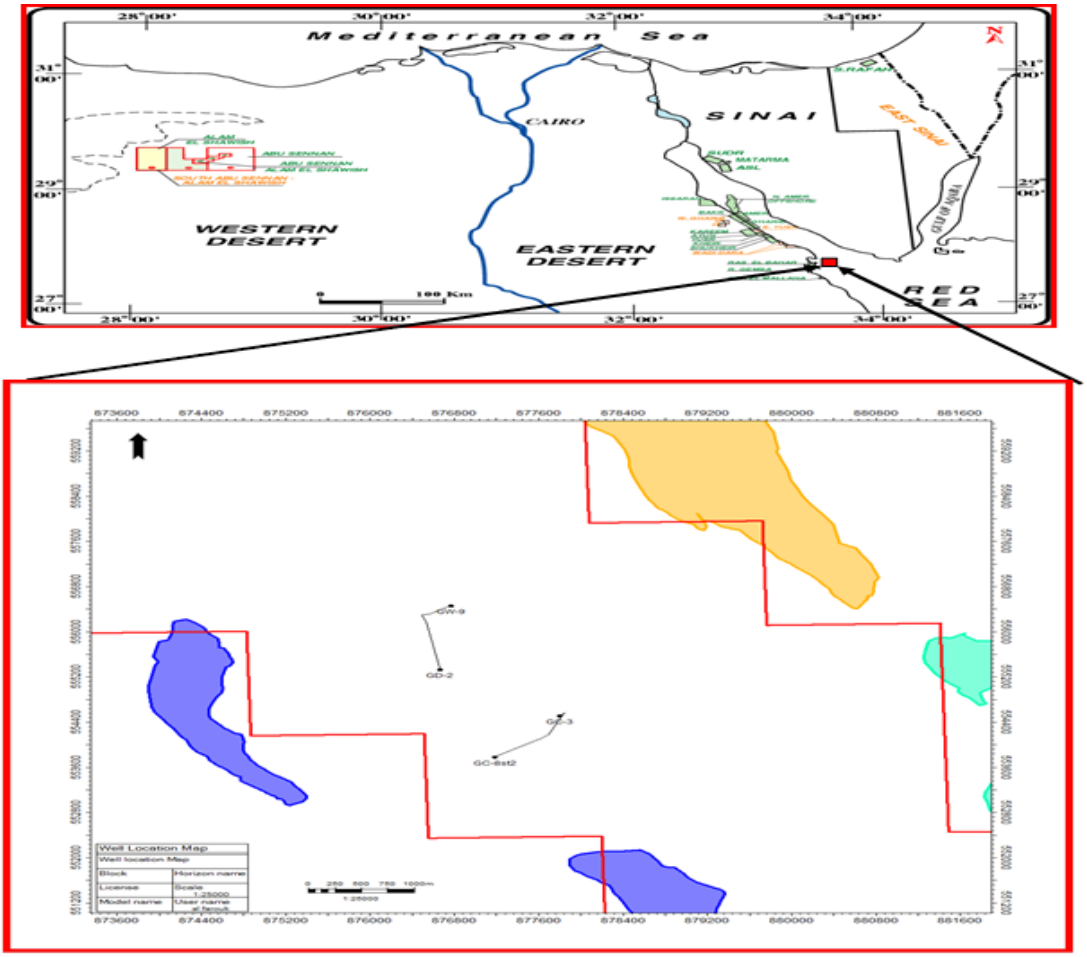

Fig. 1: Base map of the studied wells in North Geisum oil Field, Gulf of Suez Egypt.

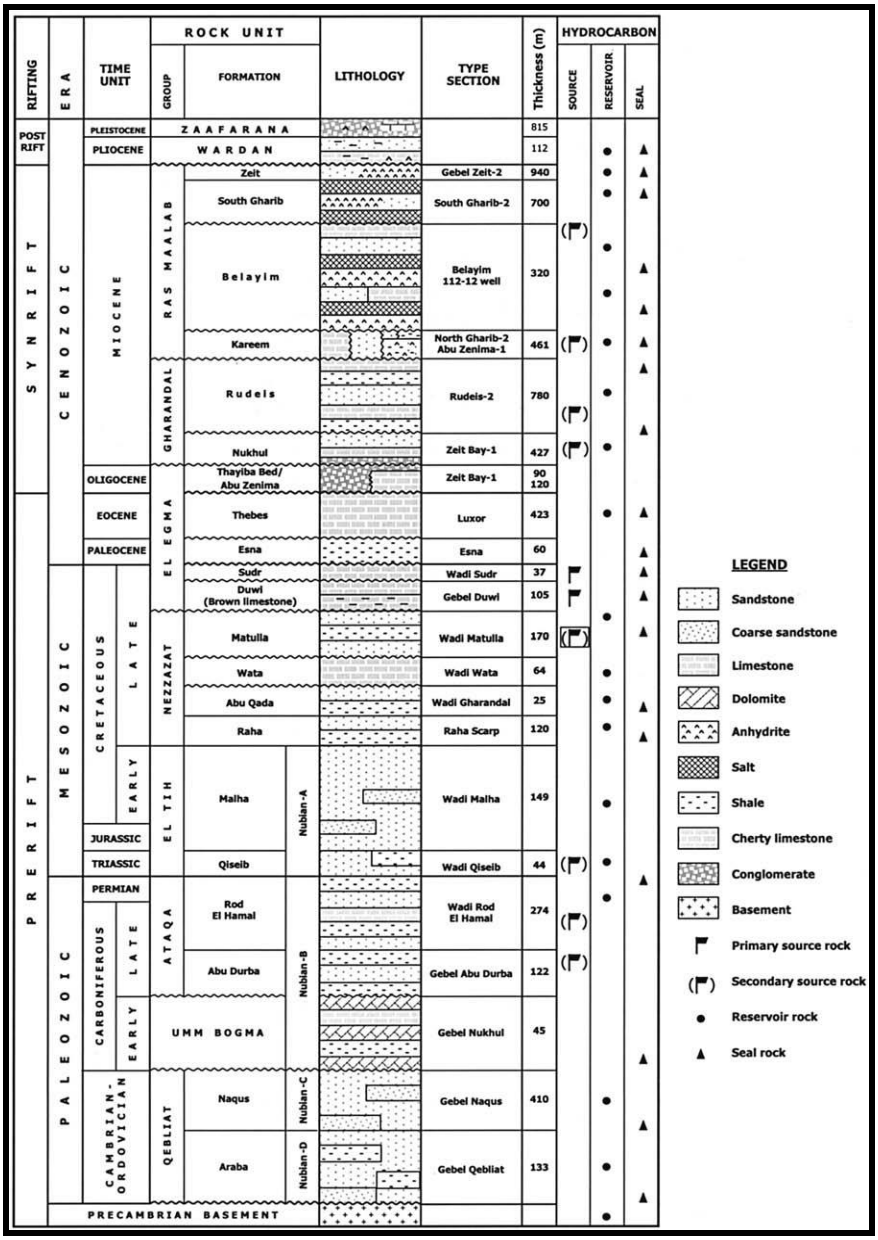

Fig. 2: Generalized stratigraphic column of Southern Gulf of Suez, Egypt (Alsharhan, 2003).

The Gharandal Group comprises (from base to top) the Nukhul, Rudeis and Kareem Formations. These Miocene rocks are unconformably underlain by Paleozoic to Mesozoic Sandstone of Nubia facies which cover unconformably the Precambrian basement rocks.

The Kareem Formation was introduced by the EGPC Stratigraphic Committee (1964) to describe the uppermost rock unit of the Lower to Middle Miocene Gharandal Group. The Kareem Formation is bounded by two unconformities separated it from the underlying open marine Rudeis Formation and the overlying Belayim Formation that was deposited in greatly fluctuating depositional environments.

The EGPC committee (1964) divided the Kareem Formation in the study area into two unconformably members. The lower Member is known as the Rahmi Member which is made up of thin beds of anhydrite intercalated with sandstone, shale and carbonate rocks. The depositional setting of the Rahmi Member was shallow, partly open marine, with lagoonal conditions. The upper member is termed Shagar Member that consists of interbedded shale, limestone and sandstone. It was deposited in deep inner to shallow outer sublittoral setting. The boundary two members are defined by the first appearance of anhydrite (Tewfik et al., 1992).

The Rudeis Formation conformably overlies the Nukhul Formation and is disconformably overlain by Kareem Formation. It varies greatly in lithology, thickness and depositional setting, in response to their irregular paleo-relief over which sedimentation took place (Tewfik et al., 1992). The Rudeis Formation consists mainly of shale and limestones that are interbedded with sandstone.

The Rudeis Formation was subdivided into four members which are (from base to top): Bakr, Yusr, Safra and Ayun members. Several operating oil companies have further subdivided the Rudeis Formation. Most companies have subdivided the Rudeis Formation into two units (lower and upper). The lower unit (Late Aquitanian) is made up of mixed siliciclastic rocks (light brown calcareous shale and highly calcareous sandstone, partially glauconitic) and few streaks of limestone (Samir, 2012).

The upper unit (Burdigalian) consists mainly of light brown calcareous shale, partially glauconitic and rich in planktonic and benthonic foraminifera, argillaceous limestone and gritty sandstone. The depositional environment of the Rudeis Formation is alternating between shallow and deep marine (Balduzzi et al., 1978; Said, 1990; El Beialy and Ali 2002 and Amgad, 2011).

4-Structure Setting of the Gulf of Suez

The evolution of interior basin Gulf of Suez is illustrated in (Fig. 3) in stages from the Paleozoic to the Holocene and is characterized by tectonic extensional events producing tension block faulting (horst and graben) and block subsidence (see also Kingston et al., 1983). Thus the Gulf of Suez has developed in a series of distinct evolutionary stages.

(1) In the first stage, Paleozoic terrestrial clastics were deposited over Precambrian crystalline basement affected by minor tectonic movements. The Hercynian epeirogeny folded and uplifted the Paleozoic deposits. The hiatus caused by these movements is evident in the thinning or absence of sedimentation in many parts of the Gulf of Suez, where Cenomanian strata rest unconformably on Carboniferous strata.

(2) The second stage occurred during the Permian–Triassic to Jurassic and is characterized by local subsidence and minor transgression, leading to deposition of fluviomarine red shales and sandstones.

(3) The third stage dates from the Early Cretaceous and involved rifting of the continental crust, under tension, to produce a system of grabens via block faulting. Depressions were later filled with nonmarine sandstone and shale.

(4) During the fourth stage, which extended from the middle Cretaceous to the Miocene, normal faulting continued and the graben system gradually subsided to form a deep basin. Early and middle Alpine movements occurring in this stage had significant effects on the structure of Mesozoic and Paleogene strata and gave rise to a series of folds in areas of tectonic compression. Marine waters invaded the basin and deposited a range of different sedimentary facies, varying with location in the basin. Marine sandstone and shallow marine limestone, including reefal limestone, were deposited on structural highs, whereas shale and globigerinal marl accumulated in the low areas. The last strata of this stage were thick salt deposits.

(5) During the fifth and final stage of rift evolution, the interior fracture system widened during the Pliocene–Holocene, the basin fill was uplifted at the rift margins because of continued block faulting and nonmarine wedge top strata (mainly sandstone) penetrated the basin.

Table 1: Average Values of petrophysical parameters of pay zones for the different Beds in North Geisum oil field.

Wells	Member	Beds	Parameters						
			Vsh	PHIT	PHIE	Sw	Sh	Gross Thickness	Net Thickness
GC-3	SHAGAR	Shagar Cap	21	20	18	44	56	78	25
		Shagar Sand	5	19	18	23	77	32	29
	RAHMI	Rahmi Clastics	17	14	14	41	59	15	8
		Rahmi Sand	5	18	18	44	56	32	25
GD-2	SHAGAR	Shagar Cap	22	13	12	42	58	10	6
		Shagar Sand	6	18	18	16	84	61	61
	RAHMI	Rahmi Clastics	10	15	15	39	61	55	28
		Rahmi Sand	11	18	18	27	73	128	117
GC-8ST2	SHAGAR	Shagar Cap	16	23	22.5	44	56	572	56
		Shagar Sand	16	15	15	32	68	108	63
	RAHMI	Rahmi Clastics	13	18	18	45	55	275	41
		Rahmi Sand	ABS	ABS	ABS	ABS	ABS	ABS	ABS
GW-9	SHAGAR	Shagar Cap	12	26	19	27	73	25	12
		Shagar Sand	13	16	16	40	60	38	32
	RAHMI	Rahmi Clastics	7	18	18	43	57	126	47
		Rahmi Sand	ABS	ABS	ABS	ABS	ABS	ABS	ABS
NOTE	ABS: Absent								

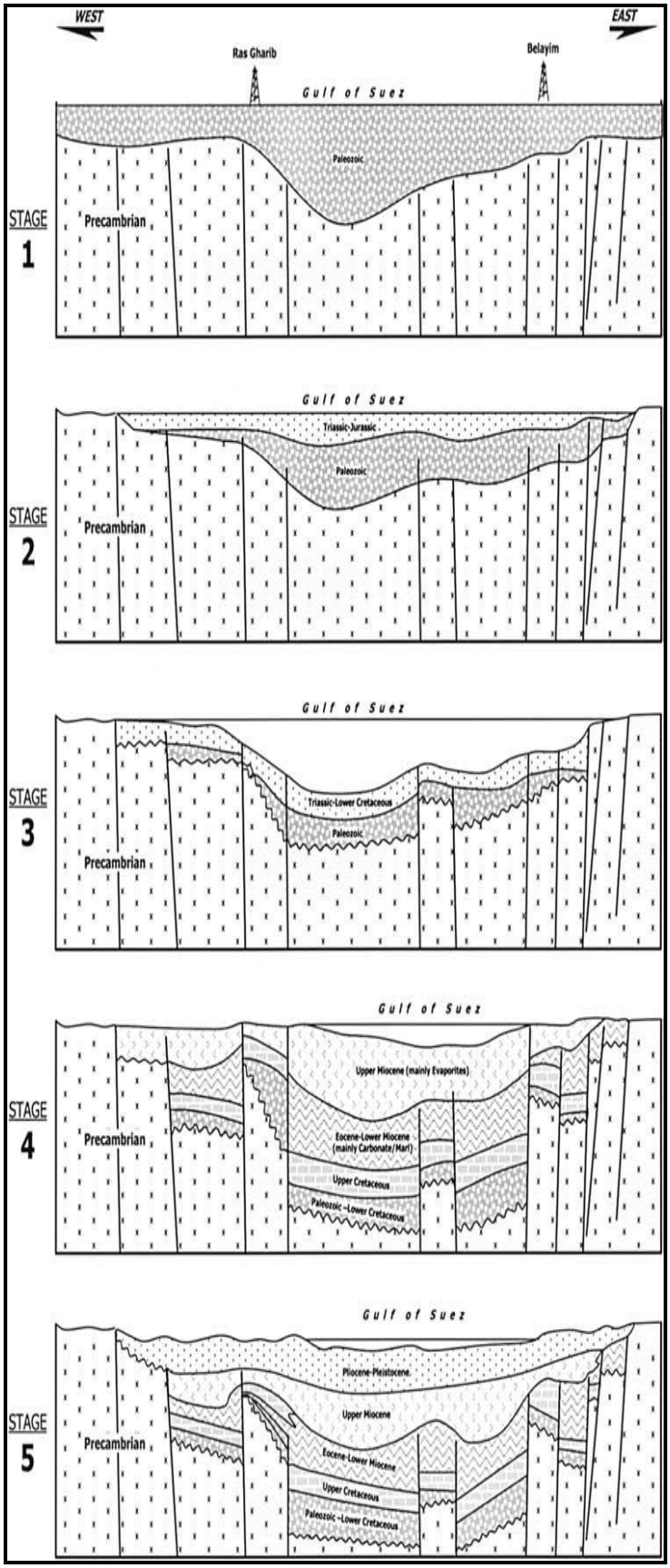

Fig. 3: Development stages of the Gulf of Suez, as an example of a typical interior fracture rift basin (stages 3–5 modified from Kingston et al. [1983]).

5- Petrophysical analysis

The petrophysical and hydrocarbon characteristics of Shagar and Rahmi members are based mainly on the well log analysis of four wells, which are distributed through in southern Gulf of Suez in the North Geisum oil field (Fig. 1). A number of petrophysical plots are constructed for the studied wells. These plots are the final layout that collects the different deduced petrophysical parameters, of prime interest, together and allow their interpretation vertically with depth. Additionally, a number of distribution maps are constructed for Intra Shagar Cap, Shagar Sand and Intra Rahmi Clastics reservoirs such as total porosity, effective porosity, volume of shale and hydrocarbon saturation maps.

A) Vertical Distribution of Petrophysical Parameters

I- Shale Volume (Vsh)

The accurate determination of shale volume (V_{sh}) is very important for reservoir rocks analysis. The determination of reservoir quality in terms of petrophysical parameters, lithology identification, porosity, type and distribution of fluids and anticipated water cut estimates these parameters are all of primary importance to the proper evaluation of reservoir potentiality**.**

Shale volume is calculated from multiple clay indicators. It is either from single curve (e.g. gamma ray), and deep resistivity responses (RESD), alternatively two curves (e.g. sonic/neutron, neutron/density, and sonic/density) curves.

The determination of the shale parameters (ΦN_{sh}, ρ_{sh}, ΔT_{sh} and Rt_{sh}), often depends on the experience of the log analyst since such parameters vary according to different geological factors. These parameters can be calculated directly from the composite log or through constructing a number of frequency crossplots.

II-Determination of Formation Porosity (φ)

The formation porosity is very important parameter for formation evaluation in quantitative well log analysis. Porosity is the percentage of voids to the total volume of rock. It is measured as a percent and has the symbol ϕ. The amount of internal space or voids in a given volume of rock is a measure of the amount of fluids a rock holds. The four types of porosity (total, primary, secondary and effective porosities) can be determined by using porosity logs (density, sonic and neutron) or by combination of them (Figs. 6, 7).

III- Determination of fluid saturations

Several interpretation techniques are used for determining the fluid saturation. In all cases, the first step is to determine the type of fluids occupied in the pore space and to differentiate them into water and hydrocarbons (oil or gas). When the pore spaces are partially saturated with water, the remainder will be occupied by oil or gas (Figs 8, 9).

Because oil and gas are nonconductors, the resistivity of the rock partially saturated with hydrocarbons (Rt) is higher than the resistivity of the same rock when fully saturated with water (Ro).

IV- LITOSATURATION CROSS PLOTS

It is very important to study the vertical changes of the sedimentation patterns within genetically related stratigraphic units because they reflect differences in both local environment and tectonic framework of that unit. The study of the vertical changes of stratigraphic unit helps in hydrocarbon evaluations (Figs 10, 11).

1-Litho-Saturation Crossplots of GC-3 Well

A Litho-saturation crossplots and data logs is displayed for the interval 4774 ft. to 5428 ft. (Fig.10) where Kareem Formation in the study area is subdivided into Shagar and Rahmi beds from top to bottom respectively. The Shagar bed is divided into Shagar Cap and Shagar Sand. Shagar Cap is dominated by shale with streaks of limestone and contains marine sand body interbedded called Intra Shagar. The gross thickness is 78 ft. Shale content is high where reaches its maximum value at middle, while decreases toward the upper and lower parts. The average shale volume of this formation is about 21%, the average total porosity of this formation is about 20 %, the effective porosity 18%, water saturation 44 % and hydrocarbon saturation 56%. It is considered as a good reservoir.

Shagar cap followed by sand body with limestone and shale streaks called Shagar Sand bed where its gross thickness is 32 ft. The average shale volume about 5 %, the average total porosity about 19% and the effective porosity 18%, water saturation 23% and hydrocarbon saturation 77 %. It is considered as good reservoir; especially in the parts of high porosity.

The Rahmi Member divided into Rahmi Anhydrite, Rahmi Clastics and Rahmi Sand beds.

Rahmi Anhydrite consists of anhydrite with thickness 50 ft. and followed by Rahmi Clastics bed.

Rahmi Clastics bed composed of shale, limestone and streak of sand called intra Rahmi Sand. Its gross thickness 15 ft. The average shale volume about 17 %, the average

total porosity about 14 %, and the effective porosity 14% water saturation 41% and hydrocarbon saturation 59%. It is considered as a good reservoir; especially in the parts of high porosity.

In the lower part of Kareem Formation there is thick sandstone called Basal Rahmi Sand bed. Its gross thickness is 32 ft. The average shale volume of this bed about 5 %, the average total porosity about 18% and the effective porosity 18%, water saturation 44% and hydrocarbon saturation 56 %.

GC-3 well is considered as good reservoir due to good PHIE and hydrocarbon saturation which is affected by the migration of hydrocarbon through normal fault.

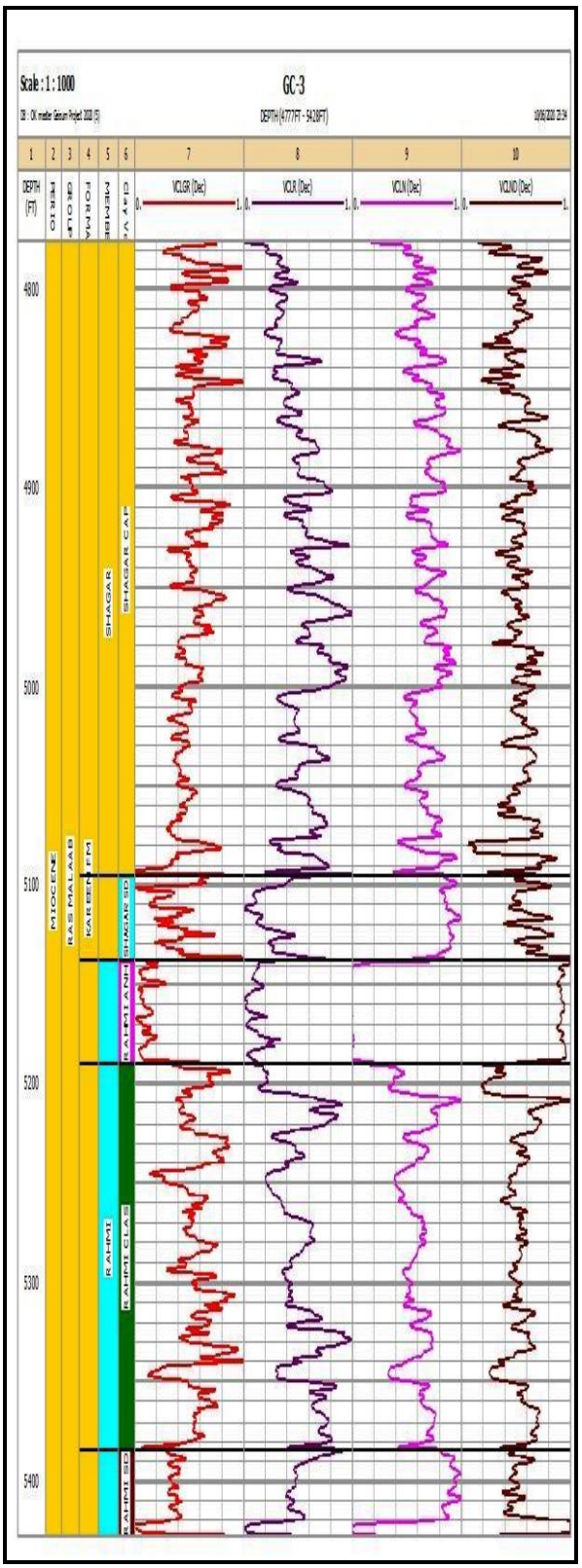

Fig. 4: Presentation showing calculated Shale volume of GC-3 well by using IP program software.

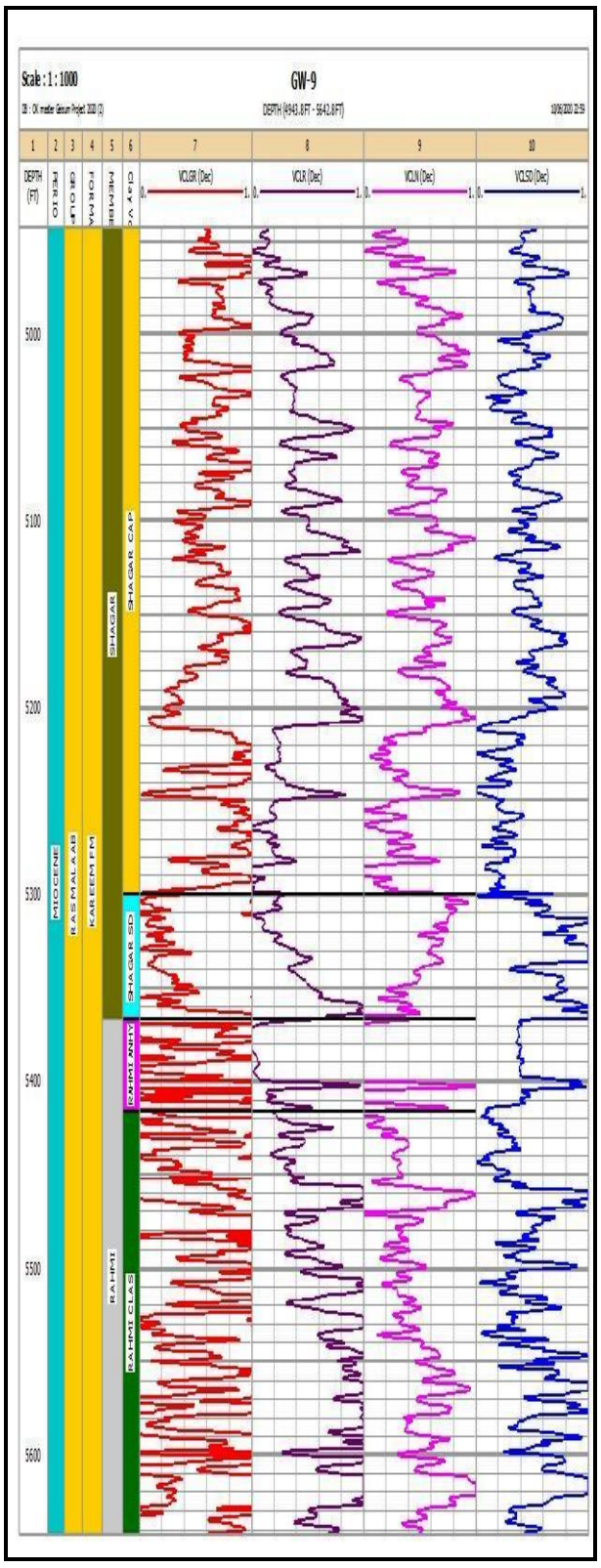

Fig. 5 Presentation showing calculated Shale volume of GW-9 well by using IP program software.

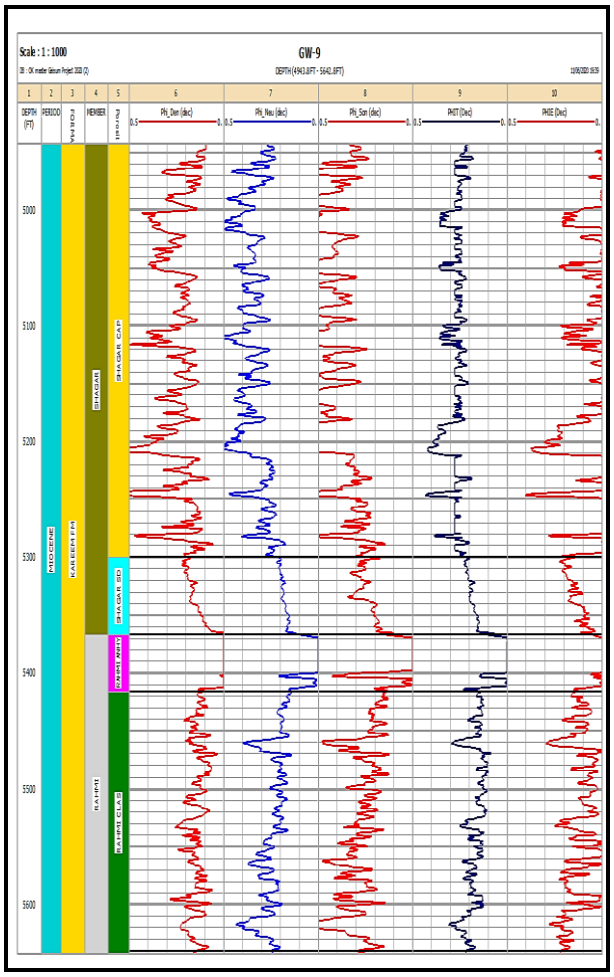

Fig. 6: Presentation showing calculated porosity of GC-3 well by using IP program software.

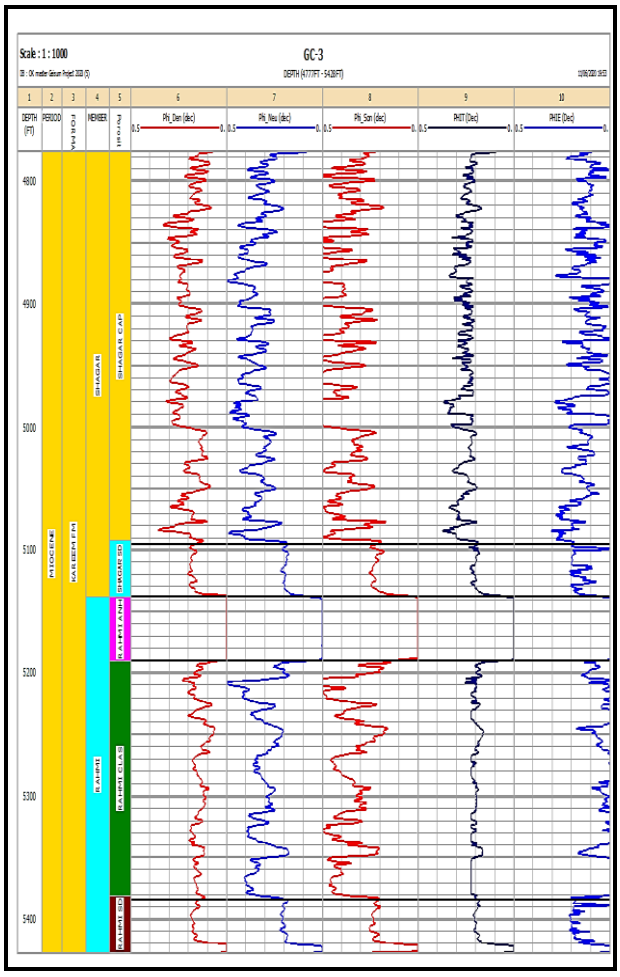

Fig. 7: Presentation showing calculated porosity of GW-9 well by using IP program software.

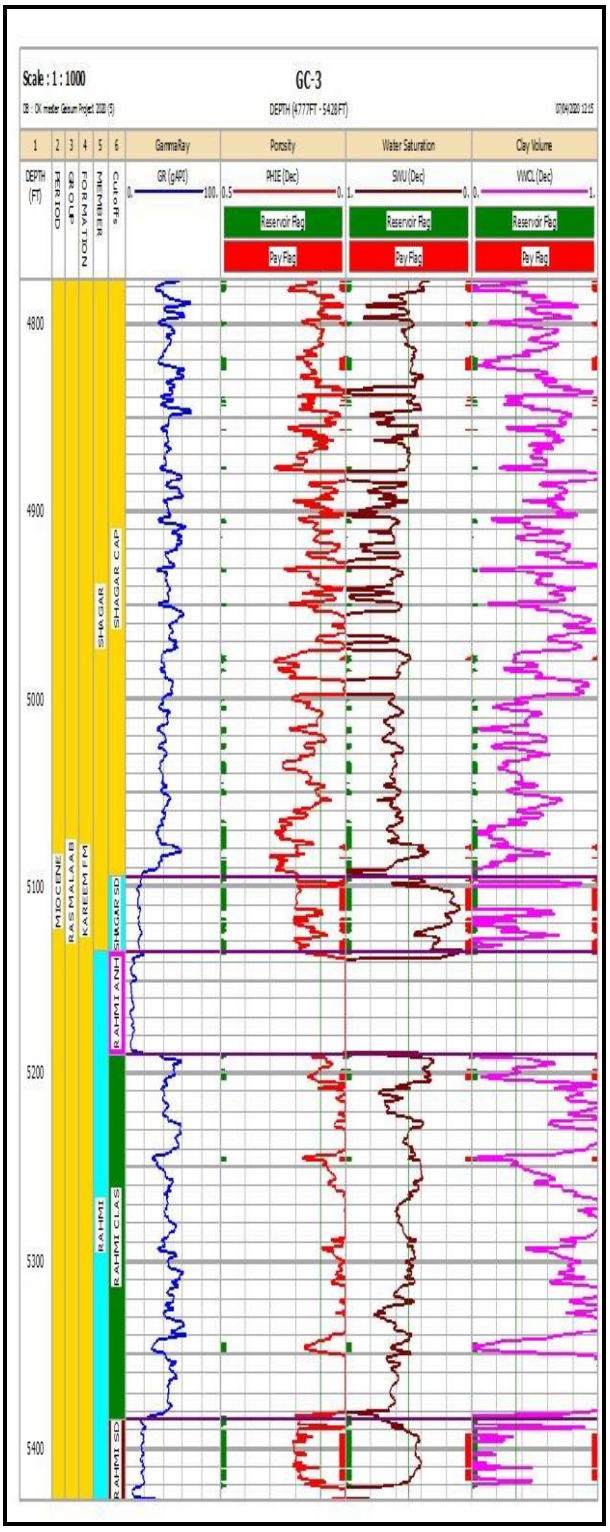

Fig. 8: Presentation showing calculated fluid GC-3 well by using IP program software.

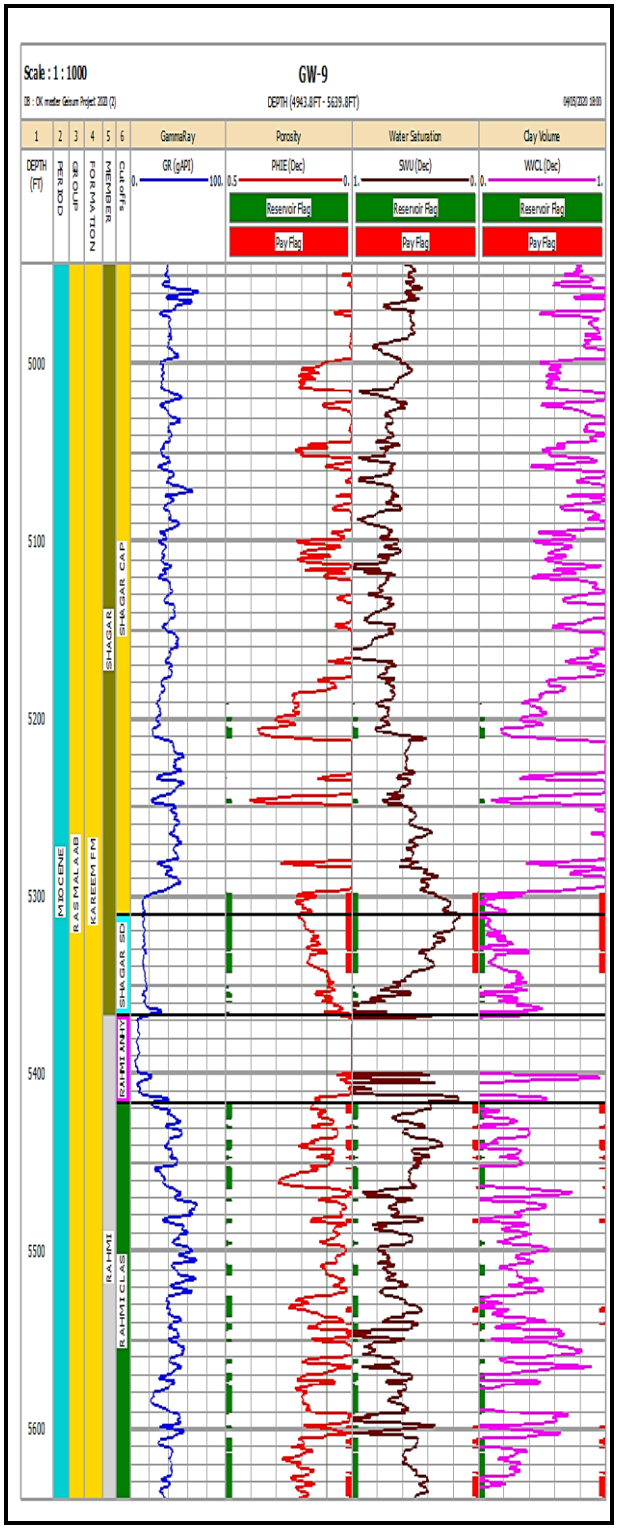

Fig. 9: Presentation showing calculated fluid saturation of GW-9 well by using IP program software.

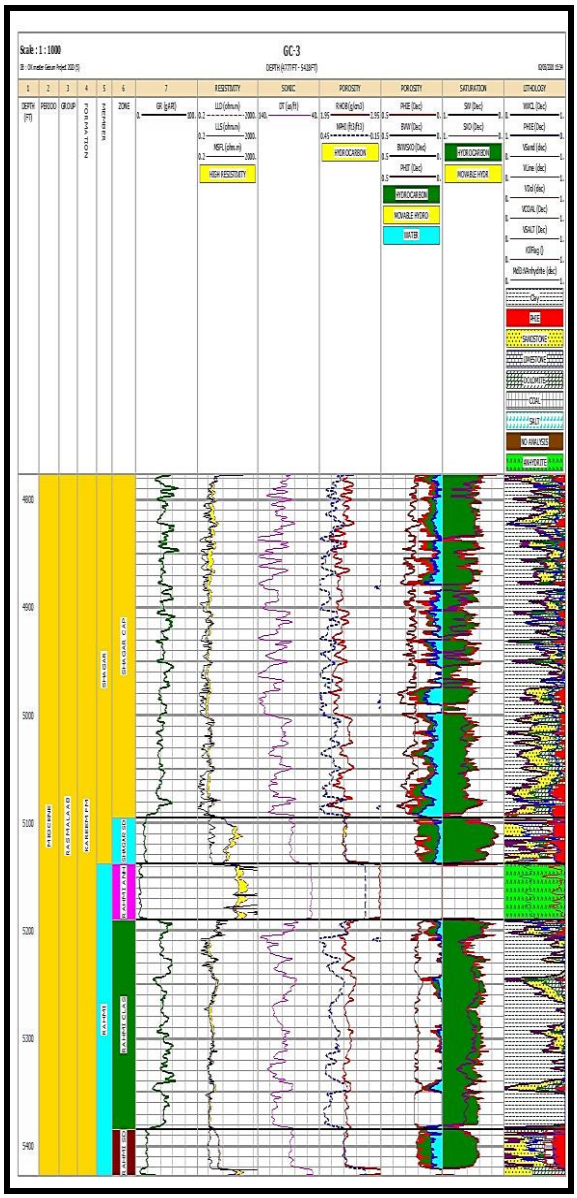

Fig. 10: Litho saturation cross plot of GC-3 well.

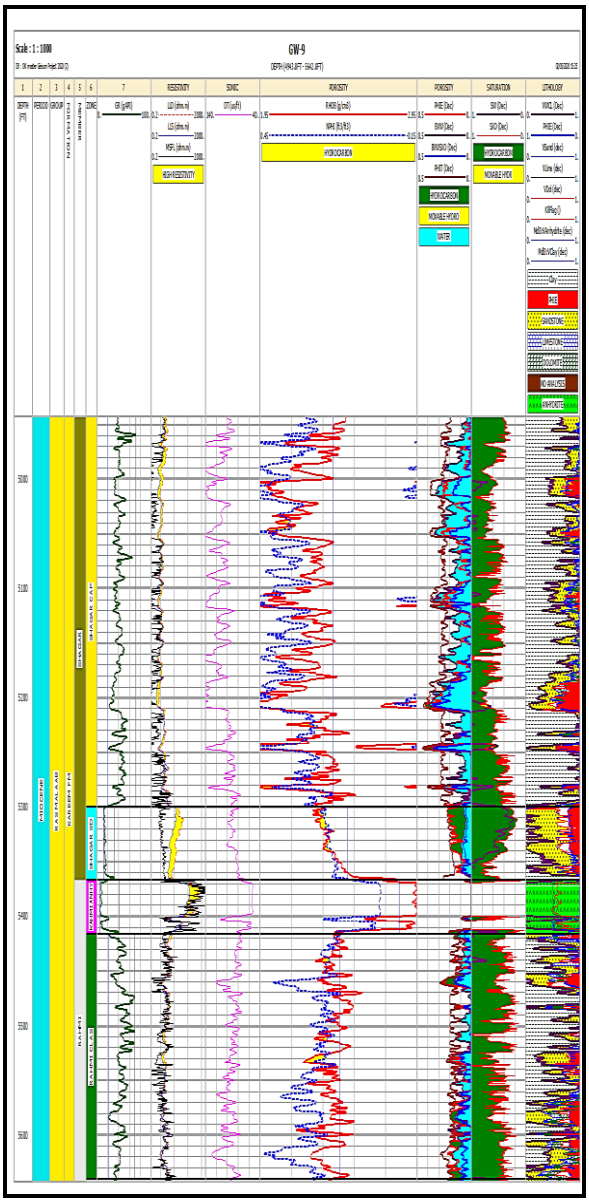

Fig. 11: Litho saturation cross plot of GW-9 well.

The parameters used in this study include volume of shale, total porosity, effective porosity and fluid saturation where their average values are tabulated in Table (1).

2-Litho-Saturation Crossplots of GW-9 Well

A litho-saturation crossplots and data logs display for the interval 4944 ft. to 5640 ft. This well is constituted from the Shagar Cap, Shagar Sand, Rahmi Anhydrite, Rahmi Clastics and Rahmi Sand beds. The litho-saturation cross plot is shown in (Fig. 11) in GW-9 well shows that Kareem Formation in the study area is subdivided into Shagar and Rahmi Members from top to bottom respectively. The Shagar Member is divided into Shagar Cap and Shagar Sand beds.

Shagar Cap is dominated by mainly shale with limestone and sandstone streaks called Intra Shagar sand. Gross thickness of Shagar Cap is 25 ft. The average shale volume of about 12 %, the average total porosity 26 %, the effective porosity 19%, water saturation 27% and hydrocarbon saturation 73%. It is considered as good reservoir.

Shagar Cap is followed by sand body called Shagar Sand with 38 ft. as Gross thickness and the average shale volume is about 13 %, the average total porosity of this bed is about 16 %, the effective porosity 16%, water saturation 40% and hydrocarbon saturation 60 %.

On the other hand, the Rahmi Member is divided into Rahmi Anhydrite, Rahmi Clastics and Rahmi Sand beds. Rahmi Anhydrite's thickness is 49 ft. and consists of anhydrite followed by Rahmi clastics which consist of mainly shale, sandstone with limestone streaks. The average shale volume of this formation is about 7 %, the average total porosity 18 %, the effective porosity 18%, water saturation 43% and hydrocarbon saturation 57%.

GW-9 well is affected by the absence of Rahmi sand bed due to erosion or non-deposition and is considered as good reservoir due to good PHIE (16%-19%) and hydrocarbon saturation (57%-73%).

GW-9 well is affected by horst and three way dip closure fault which is considered as structural trap for hydrocarbon accumulation and increase of hydrocarbon saturation effect.

The parameters used in this study include volume of shale, total porosity, effective porosity and fluid saturation (water saturation and hydrocarbon saturation). Their average values are tabulated in Table (1).

B)- Lateral distribution of petrophysical parameters

Lateral distribution of the petrophysical parameters of interest was enhanced in the present study, especially for those parameters concerning with hydrocarbon potentialities. Accordingly, a number of property distribution maps were constructed for Shagar Cap, Shagar Sand, Rahmi Clastic and Rahmi Sand reservoirs such as total porosity, effective porosity, volume of shale, water saturation and hydrocarbon saturation maps.

I-The Total Porosity Distribution Maps

The total porosity distribution map of the Shagar Cap (Fig. 12) shows an increase towards the northwest direction, with a maximum value (26 %) at the GW-9 well and a minimum value (13 %) at the GD-2 well.

Figure (13) exhibits the total porosity distribution map of the Shagar Sand Bed in which there is an increase of total porosity toward the east direction, with a maximum value (19%) at the GC-3 well and minimum value (15%) toward south of the study area at the GC-8ST2 well.

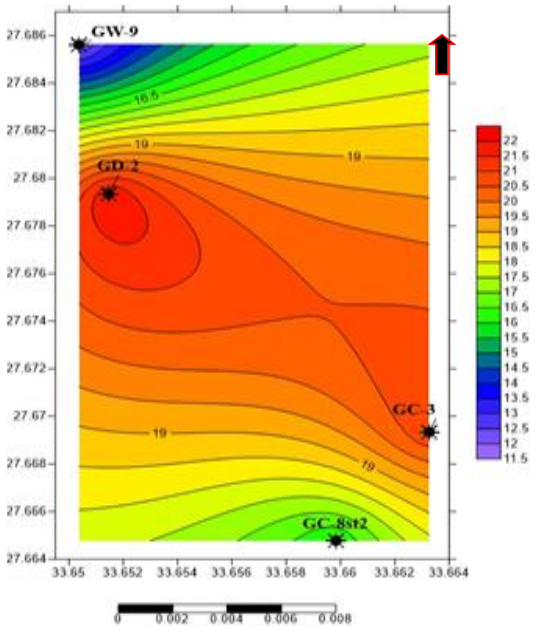

Fig. 12: Total Porosity distribution map of Shagar Cap bed.

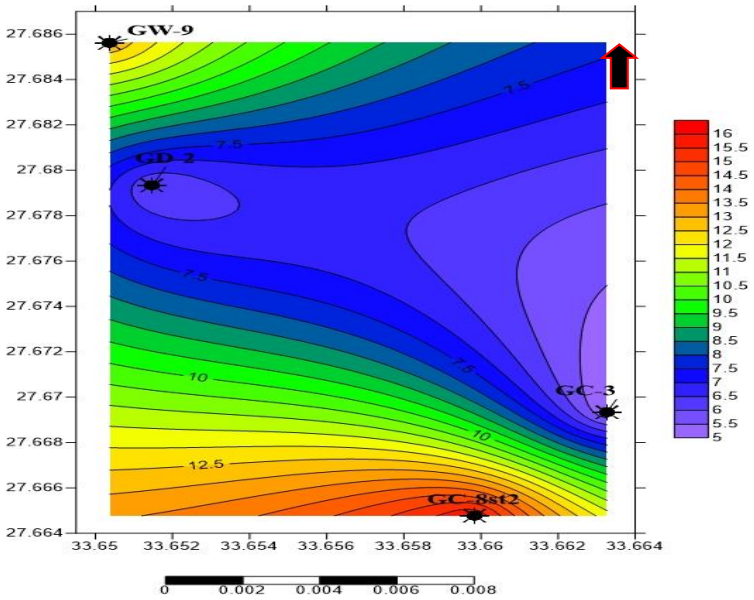

Fig. 13: Total Porosity distribution map of Shagar Sand bed.

Figure (14) illustrates the total porosity distribution map distribution map of the Rahmi Clastic bed. It shows an increase of total porosity toward the northwest and south directions, while it decreases toward the east and west directions of the study area. The maximum value of total porosity (18%) is recorded at the GC-8ST2 and GW-9 wells and its minimum value (14%) is at the GC-3 well.

The effective porosity distribution map of pay zone of the Shagar Cap bed (Fig. 15) illustrates variation in the effective porosity values from a maximum value (22.5 %) at GC-8ST2 well to a minimum value of (12 %) at the GD-2 well. Effective porosity distribution increases toward south directions but decreases toward the west direction of the study area.

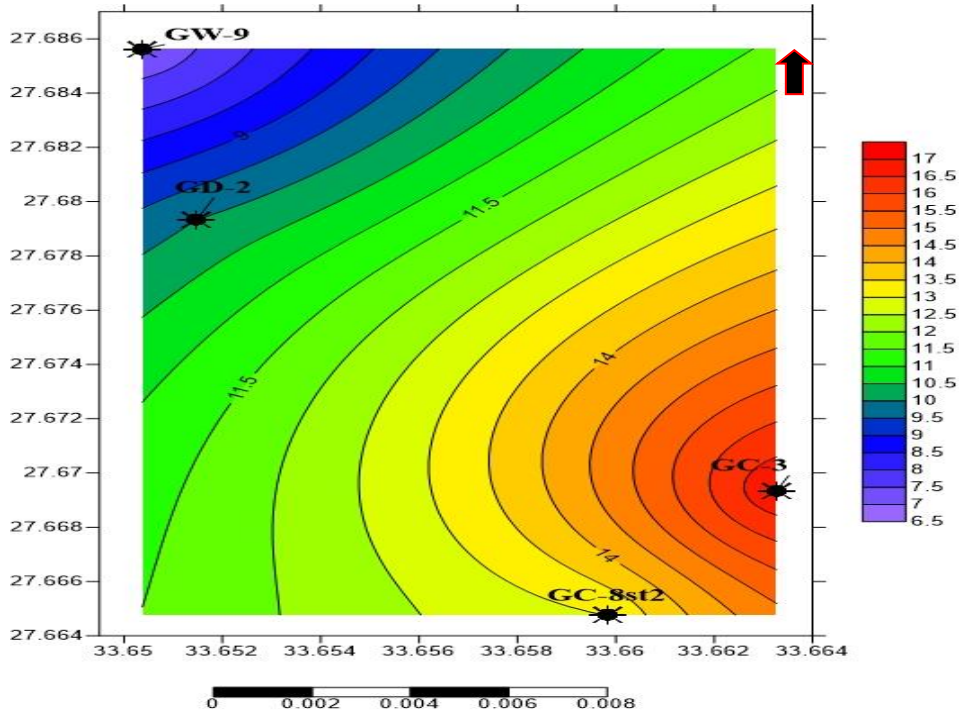

Fig. 14: Total Porosity distribution map of Rahmi Clastics bed.

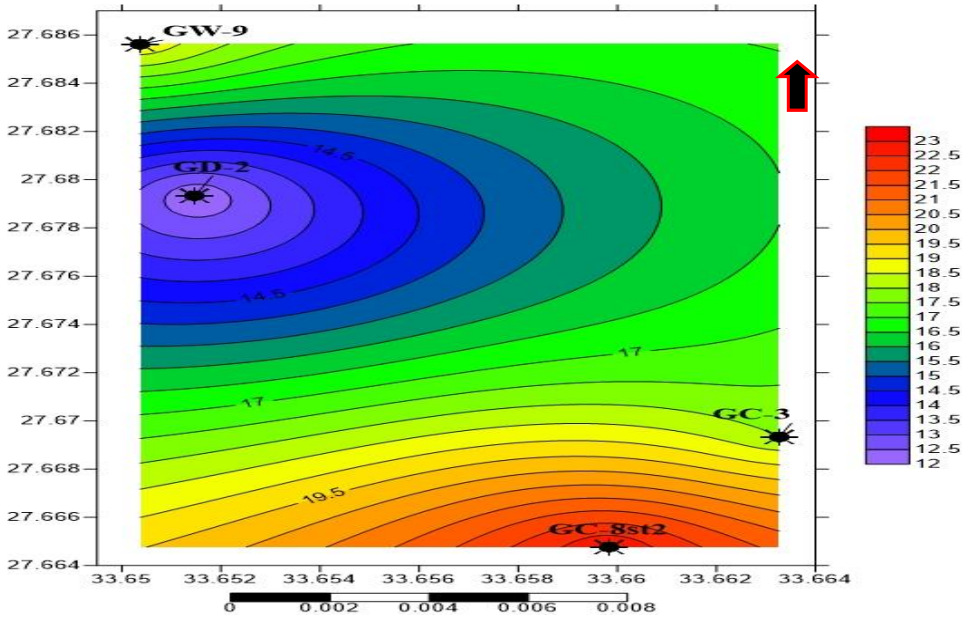

Fig. 15: Effective Porosity distribution map of Shagar Cap bed.

Figure (16) exhibits the effective porosity distribution map of pay zone of the Shagar Sand bed which increases toward the west and east directions, with a maximum value (18%) at the GC-3 and GD-2 wells and decreases toward south of the study area and recording minimum value (15%) at the GC-8ST2 well.

Figure (17) exhibits the effective porosity distribution map of pay zone of the Rahmi Clastic bed shows variation in the effective porosity values from a maximum value of effective porosity (18 %) is recorded at the GC-8ST2 and GW-9 wells to a minimum value (14 %) at the GC-3 well. Effective porosity distribution increases toward south and North West directions and decreases toward east of the study area.

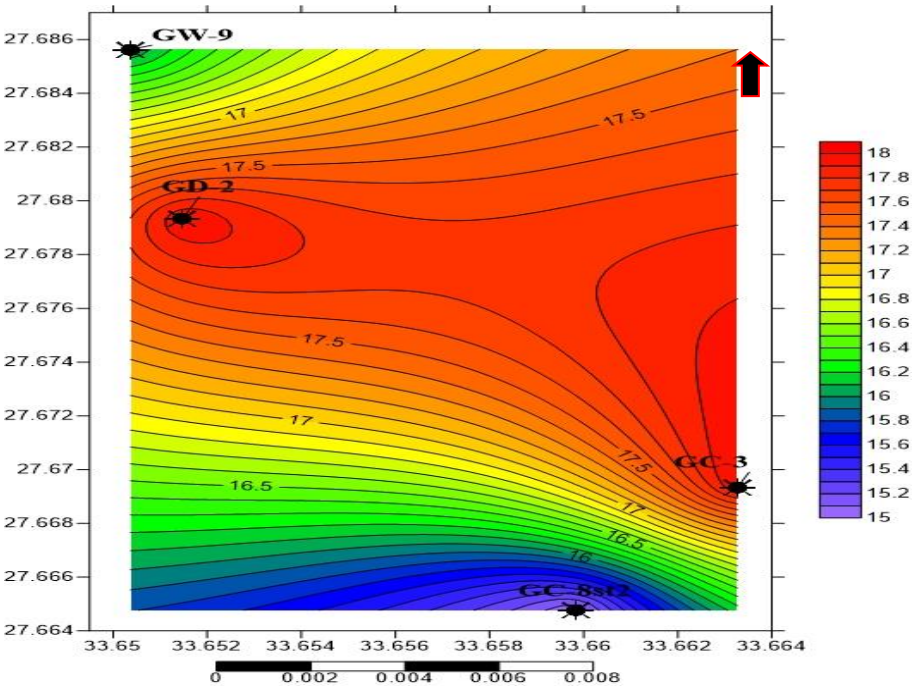

Fig. 16: Effective Porosity distribution map of Shagar Sand bed.

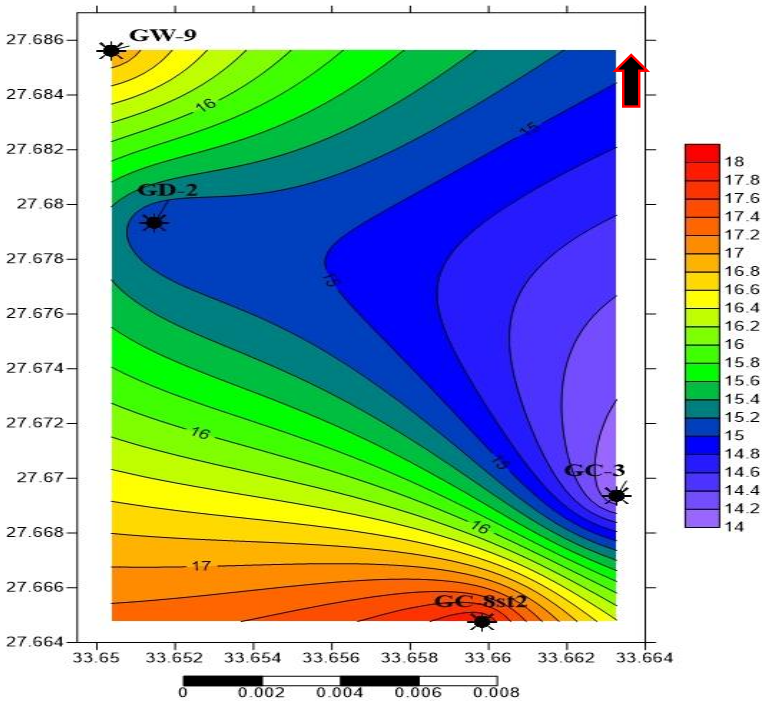

Fig. 17: Effective Porosity distribution map of Rahmi Clastics bed.

III-The Shale Volume Distribution Map

The shale volume distribution map of the Shagar Cap bed. (Fig. 18) shows variation in the shale content values. The maximum value (22 %) is recorded at the GD-2 well whereas the minimum value (12 %) occurs at the GW-9 well. Generally the shale content distribution increases toward the west direction and decreases toward the northwest of the study area.

Figure (19) illustrates the shale volume distribution map of pay zone of the Shagar Sand. It shows an increase of shale volume toward the south direction. The shale volume records a maximum value (16 %) at the GC-8ST2 well, while it decreases toward east of the study area where, the minimum value (5 %) at the GC-3 well is found.

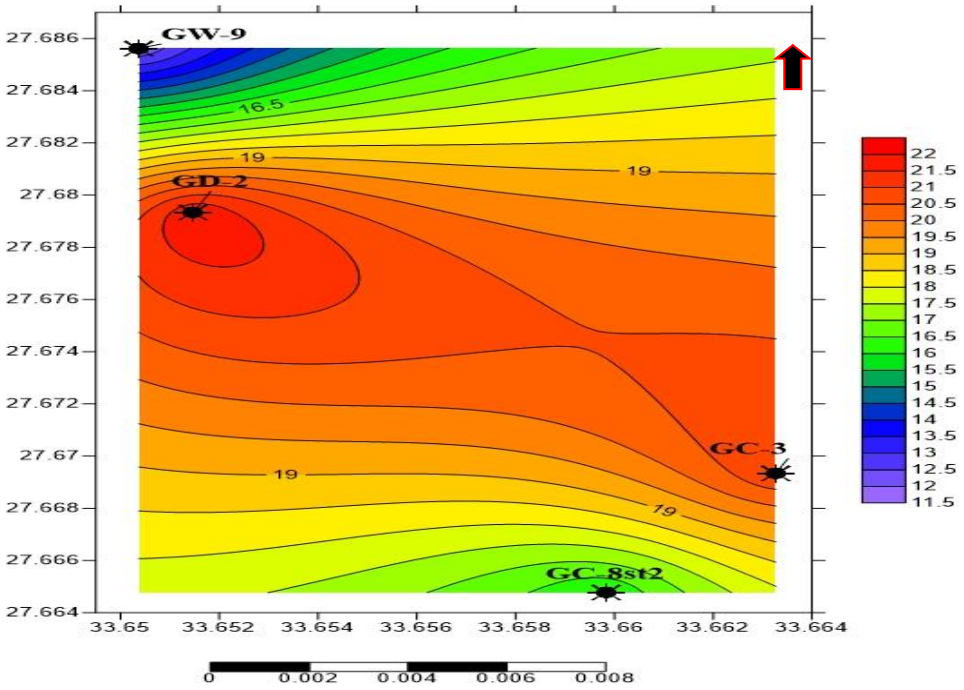

Fig. 18: Average shale volume distribution map of Shagar Cap bed.

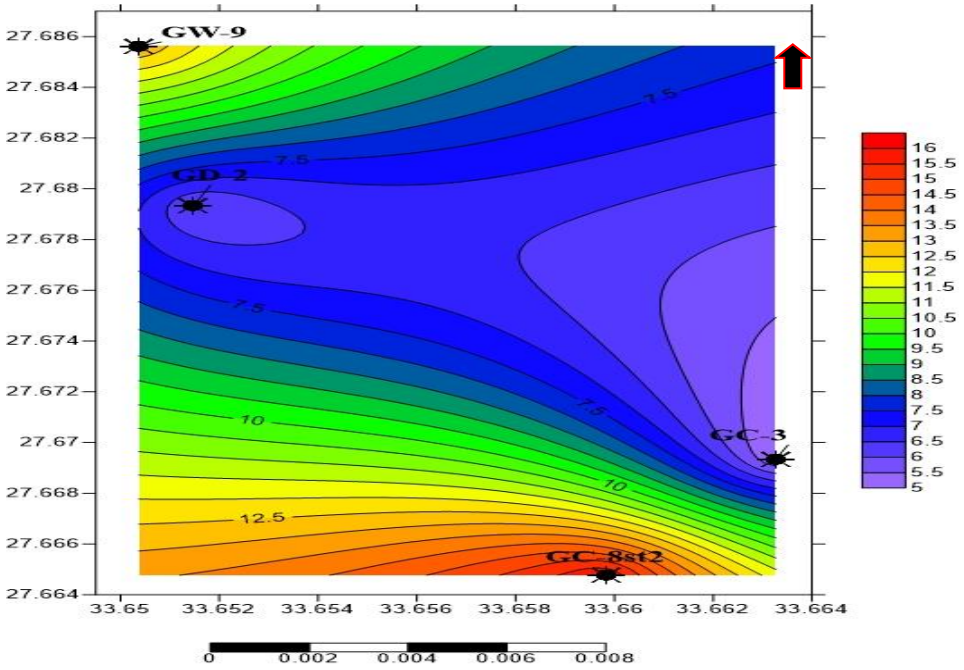

Fig. 19: Average shale volume distribution map of Shagar Sand bed.

Figure (20) The shale volume distribution map of pay zone of the Rahmi Clastic bed shows variation in the shale content values from a maximum value (17 %) at the GC-3 and minimum value (7 %) at the GW-9 well. Shale volume distribution increases toward east direction and decreases toward the northwest of the study area.

IV-The Hydrocarbon Saturation Distribution Map

The hydrocarbon saturation distribution map of pay zone of the Shagar Cap bed (Fig. 21) shows that there is variation in the hydrocarbon saturation values. The maximum value (73%) is recorded at the GW-9 well to a minimum value (56%) at the GC-3 and GC-8ST2 wells. Hydrocarbon saturation distribution increases toward the northwest direction of the study area and decreases toward the east and south directions of the study area.

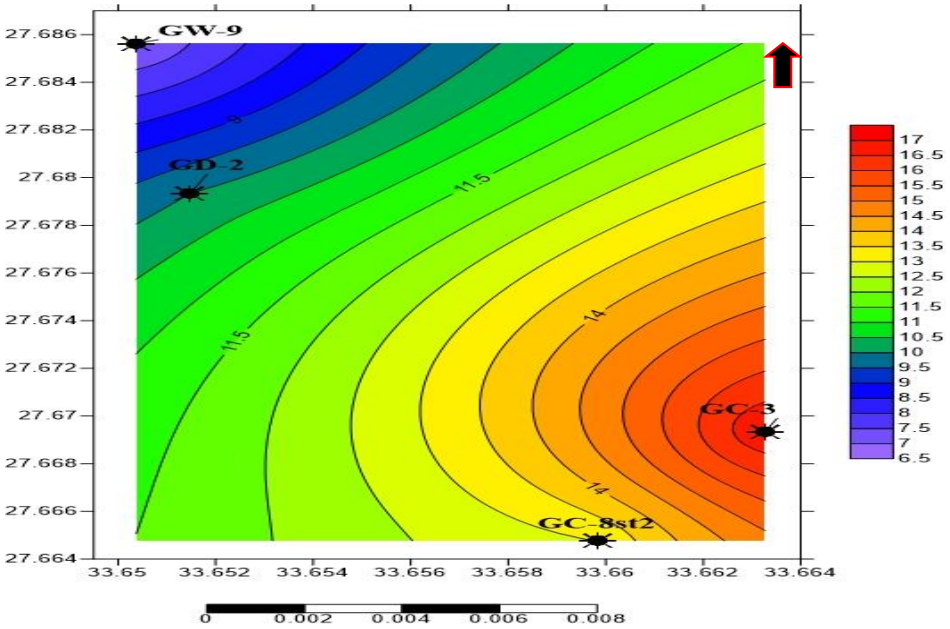

Fig. 20: Average shale volume distribution map of Rahmi Clastics bed.

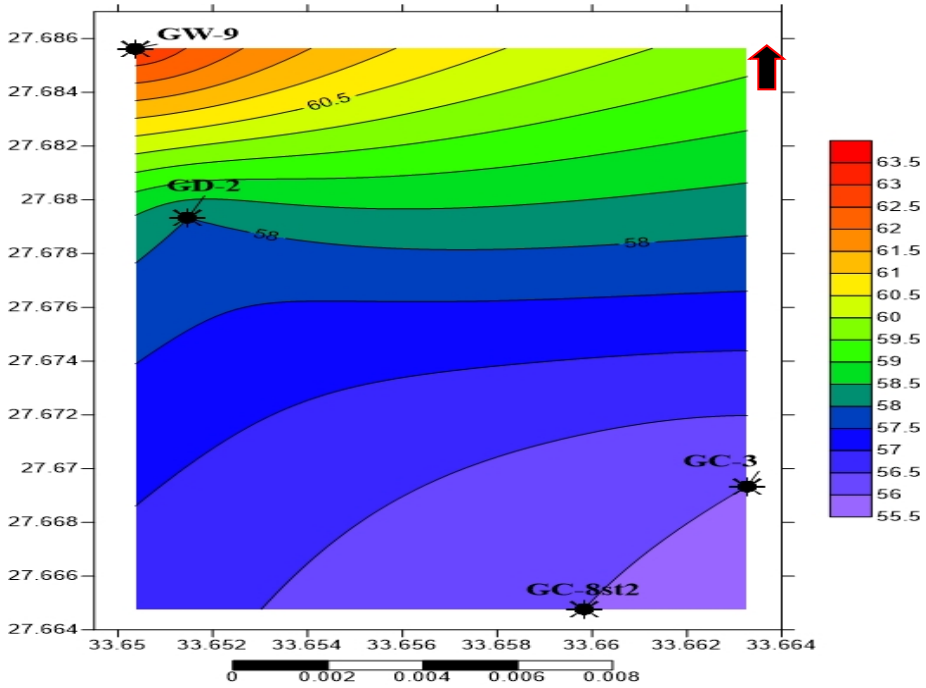

Fig. 21: Hydrocarbon Saturation distribution map of Shagar Cap bed.

Figure (22) exhibits that the hydrocarbon saturation distributions map of pay zone of the Shagar Sand Bed is increased of hydrocarbon saturation toward west direction recording a maximum value (84 %) at the GD-2 well and is decreased toward North West direction of the study area. Hydrocarbon saturation records the minimum value (60 %) at the GW-9 well.

Figure (23) The hydrocarbon saturation distribution map of pay zone of the Rahmi Clastic Bed reveals variation in hydrocarbon saturation values from a maximum value (61 %) at the GD-2 well to a minimum value (55 %) at the GC-8ST2 well. Hydrocarbon saturation distribution increases toward west direction and decreases toward the south direction of the study area.

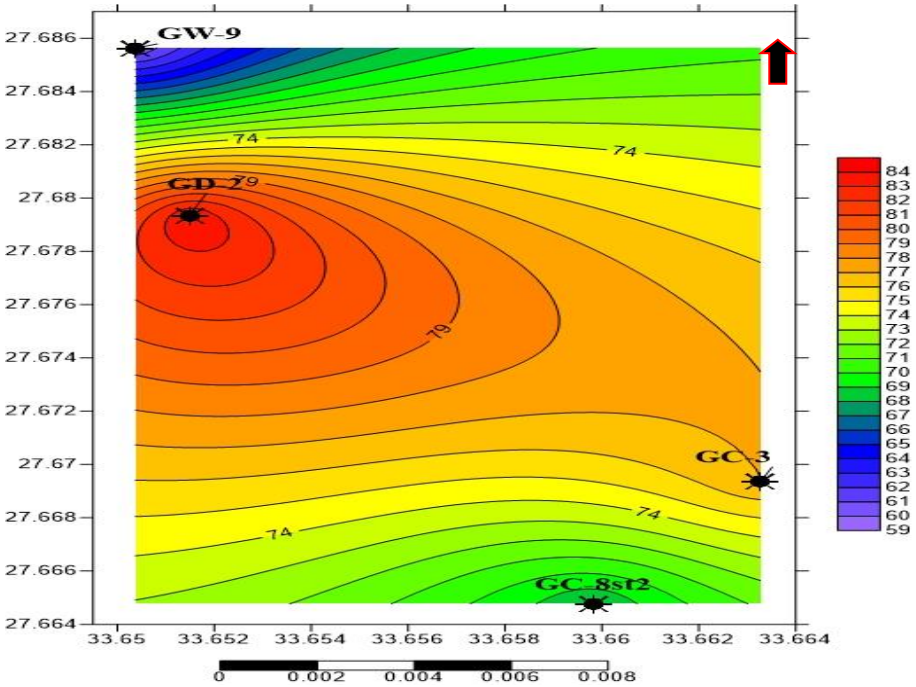

Fig. 22: Hydrocarbon Saturation distribution map of Shagar Sand bed.

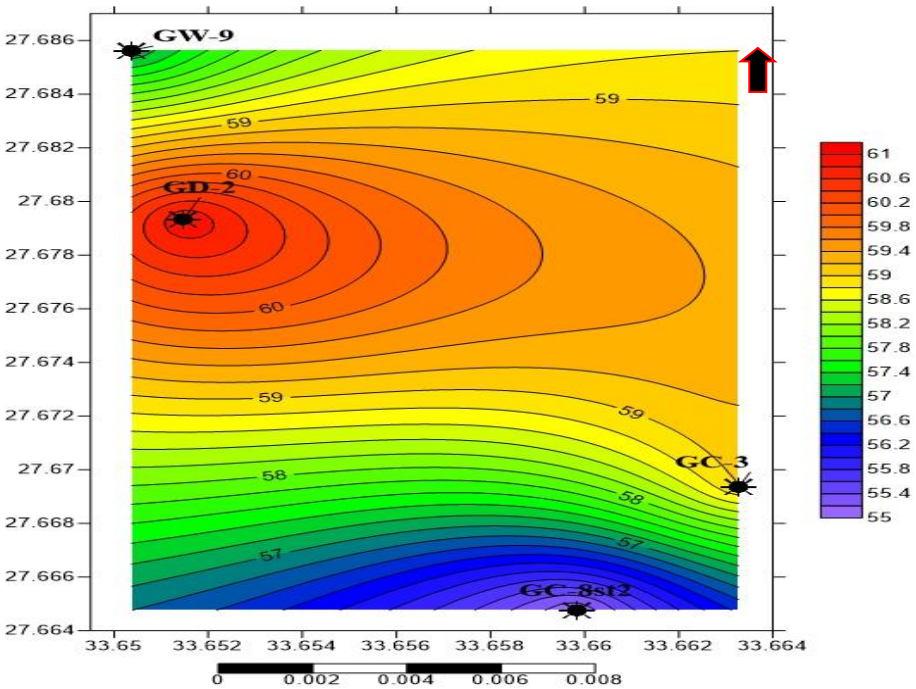

Fig. 23: Hydrocarbon Saturation distribution map of Rahmi Clastic bed.

CONCLUSIONS

In the North Geisum oil field, the most significant reservoir rocks are in the strata of the Miocene age, and the major discoveries have a principal reservoir rock of shagar cap, shagar sand and rahmi sand beds. There are many structure traps related to the faults in the study area, and there seems to be many potential traps containing hydrocarbon. Although commercial discoveries were presented, the study area is not fully understood since there are many dry wells.

Area of study affected by tectonic movement which form horst and graben on the other sides so all interested wells affected by migration of hydrocarbons by capillary movement to make area have high hydrocarbon saturation. GD-2 well consider as higher well of hydrocarbon saturation with (61% - 84%) due to effect of horst and three way dip closure fault which make good trap to accumulate hydrocarbons.

As a result of the present study, new locations are proposed to be prospects area which is located on such a three way dip closures that are very suitable place for Petroleum Accumulations.

Acknowledgments

The authors wish to express their thanks and gratitude to the EGPC (The Egyptian General Petroleum Corporation) and PetroGulf Misr Company (The General Petroleum Company) for permission and to release the data for this research.

REFERENCES

Alsharhan, A.S., 2003. Petroleum geology and potential hydrocarbon plays in the Gulf of Suez rift basin, Egypt, AAPG Bulletin, V. 87, pp. 143-180.

Amgad, S.S. 2011. Depositional model and diagenesis of the Miocene reef belt, Belayim Bay, Gulf of Suez, Egypt. M. Sc. thesis, Alexandria Uni. Egypt., 102 p.

Balduzzi, A., Cavaliere, R., Grignani, D., Lanzoni, E., Palmieri, G. and Rizzini, A. 1978. Stratigraphic and geochemical section Mediterranean Sea–Nile Delta–Gulf of Suez. Attivita Minerarie Servizio Studi Geologci E Laboratori, pp.1–23.

Egyptian General Petroleum Corporation Stratigraphic Committee 1964. Oligocene and Miocene rock stratigraphy of the Suez region. Cairo, Egyptian General Petroleum Cooperation, 142p.

El Beialy, S.Y., and Ali S.A. 2002. Dinoflagellates from the Miocene Rudeis and Kareem formations borehole GS-78-1, Gulf of Suez, Egypt. Journal of African Earth Sciences 35 (2002) pp.235–245.

Gawad, W.A.; Gaafar, I. and Sabout, A.A. 1986. Miocene Stratigraphic Nomenclature in the Gulf of Suez Region. 8th EGPC Expl. Conf. Cairo.

Kingston, D.R., C.P. Dishroon, and P.A. Williams, 1983. Global basin classification system: AAPG Bulletin, v. 67, no. 12, pp. 2175–2193.

Lashin. A., Al-Arifi N., Abu Ashour N., 2011. Evaluation of the ASL and Hawara Formations using seismic- and log-derived properties, October oil field, Gulf of Suez, Egypt. Arab J Geosci 3–4: pp. 365–383.

Said, R., 1990. The Geology of Egypt." A. A, Balkeme / Rotterdam / Brookfield. pp 1-727.

Salah, M.G., and A.S. Alsharhan, 1997. The Miocene Kareem Formation in the southern Gulf of Suez, Egypt: a review on stratigraphy and petroleum geology: Journal of Petroleum Geology, 20(3): pp. 327-346.

Samir, M.Z. 2012. Provenance, diagenesis, tectonic setting and geochemistry of Rudeis Sandstone (Lower Miocene), Warda Field, Gulf of Suez, Egypt. Journal of African Earth Sciences pp.66-67: 56–71.

Schlumberger, 1995. Well evaluation conference, Egypt: Paris, France, Schlumberger, 87 p.

Tewfik, N., C. Harwood and I. Deighton, 1992. The Miocene, Rudeis and Kareem Formations in the Gulf of Suez: Aspects of sedimentology and geohistory: 11th EGPC Exploration Seminar, Cairo, pp. 1: 84-113.